

FILTRATION OF AEROSOLS BY FIBROUS MEDIA¹

C. Y. CHEN²

Engineering Experiment Station, University of Illinois, Urbana, Illinois

Received March 5, 1955

CONTENTS

I. Introduction.....	595
II. Notation.....	596
III. Flow pattern around an isolated cylinder.....	597
IV. Collection efficiency of an isolated single cylinder.....	599
A. Collection by inertial impaction.....	599
B. Collection by direct interception.....	601
C. Collection by Brownian diffusion.....	601
D. Collection by settling.....	604
E. Collection by inertia and interception.....	604
F. Collection by diffusion and interception.....	605
G. Overall collection efficiency.....	605
H. Discussion.....	607
V. Filtration of aerosols by fibrous filters.....	607
A. Relationship between collection efficiency of fibrous filters and that of individual fibers.....	608
B. The neighboring fiber interference effect.....	609
C. Experimental results on penetration of aerosols through a filter.....	611
D. Particle size for maximum penetration.....	614
VI. Pressure drop across a fibrous filter.....	614
A. Channel theory.....	614
B. Drag theory.....	617
C. Experimental results.....	619
VII. The filtration criterion.....	622
VIII. References.....	623

I. INTRODUCTION

The problem of the removal of aerosol particles from gas streams has become of increasing importance from the standpoint of public health and the recovery of valuable products. For the removal of the large-size particles several devices, such as scrubbers and cyclones, can be used. When particles of the size of 1 micron or smaller are to be removed, fibrous filters are often used. The efficiency of collection and the pressure drop are the most important practical considerations in the design of these fibrous filters.

A filter that acts only as a sieve would give excessively high pressure drop and would have extremely high clogging rates. Practical fibrous filters have high porosity and the interfiber distances are large when compared with the size of the particles. Suspended particles may be removed from the gas stream by

¹ This paper reports work done under Contract DA18-108-CML-4789 with the Chemical Corps, U. S. Army, Washington 25, D. C.

² Present address: Yerkes Research Laboratory, E. I. duPont de Nemours and Co., Inc., Buffalo 7, New York.

direct interception, by Brownian diffusion, or by the forces of inertia, gravity, or electrical attraction. The present review will consider the case when neither the particles nor the filters are electrically charged.

As all filters are composed of individual fibers, an understanding of the mechanisms by which the particles are collected on isolated cylinders and the flow pattern around them is of fundamental importance. Discussions will then be given to show the difference between the behavior of an isolated fiber and a fiber in the filter and the relationship between the collection efficiency of a filter and that of a single fiber. As a good filter should give low resistance to flow, the theoretical and experimental work on the pressure drop across a filter is also included in this review.

II. NOTATION

- A = face area of a filter,
 B_f = fictitious film thickness,
 C = Cunningham's correction for slip flow,
 $C_D; C_{De}; C_{D\alpha}; C_{D\alpha i}$ = drag coefficients; C_D , for an isolated cylinder; C_{De} , effective coefficient for a single fiber in the filter; $C_{D\alpha}$, for a fiber with average fiber size in a filter with fiber volume fraction α ; $C_{D\alpha i}$, same as $C_{D\alpha}$ except for fiber with size d_i ,
 $C_L = \frac{v_0}{2[2.00 - \ln N_{Re}]}$,
 $C_{L\alpha}$ = drag force per unit length of fiber transverse to the flow within a filter divided by the quantity $8\pi\mu$,
 D = diffusion parameter = $\frac{D_{BM}}{v_0 d_f}$, or $\frac{D_{BM}}{v_s d_f}$, reciprocal of the Peclet number,
 D_{BM} = diffusion coefficient,
 d_b = interfiber distance, or the distance between a fiber and a boundary,
 d_f = diameter of fiber, or cylinder,
 d_f' = effective fiber diameter, as used by Davies,
 $(d_f)_{av.}$ = arithmetic average fiber diameter,
 $(d_f)_s$ = surface average fiber diameter,
 d_i = individual fiber diameter,
 d_p = diameter of aerosol particle,
 F = drag force on unit length of fiber, or cylinder,
 G = settling parameter = u_g/v_0 ,
 g = local acceleration of gravity,
 g_c = conversion factor = $980 \frac{(\text{g. mass})(\text{cm.})}{(\text{g. force})(\text{sec.}^2)}$,
 k = Boltzmann constant,
 $k_0, k_1, \dots; k_n; k'; k''$ = various constants as defined in the text,
 L = thickness of filter,
 l_i = length of fiber with diameter d_i in unit volume of filter,
 m = mass of aerosol particle,

- N, N_0 = number concentration of aerosol particles; N_0 , concentration upstream of the filter,
- $N_{Re} = \frac{d_f v_0 \rho}{\mu}$ or $\frac{d_f v \rho}{\mu}$, Reynolds number based on upstream velocity for an isolated cylinder or based on average velocity for a filter,
- Δp = pressure drop across a filter,
- Q = volumetric flow rate per unit length of fiber, or cylinder,
- R = interception parameter = d_p/d_f ,
- r_f = radius of a fiber or cylinder,
- S_0 = specific surface of a fibrous material,
- u_x, u_y = velocity components of aerosol particle in the x, y direction, respectively,
- u_g = free settling velocity of a particle,
- v = average velocity of gas in a filter, defined as v_s/ϵ ,
- v_0 = upstream velocity of gas far removed from the effect of fiber or cylinder,
- v_s = superficial velocity of gas in a filter,
- $x'; x_e; x_0$ = fluid layer thickness around a cylinder; x' at $\theta = \pi/2$ from which particles are removed by diffusion and interception; x_0 , same as x' except particles removed by diffusion only; x_e , effective thickness from which particles are removed either by diffusion or by diffusion and interception,
- Z = mobility of aerosol particles,
- α = volume fraction of fibers in a filter,
- ϵ = porosity of a filter = $1 - \alpha$,
- $\eta; \eta_0; \eta_\alpha; \eta_{\alpha i}$ = collection efficiencies of a fiber or cylinder; η_0 , for an isolated fiber; η_α , for a fiber with average fiber diameter in a filter with fiber volume fraction α ; $\eta_{\alpha i}$, same as η_α except for a fiber with size d_i ,
- λ = mean free path of gas molecules,
- μ = coefficient of viscosity of gas,
- ρ, ρ_p = densities; ρ , for gas; ρ_p for particles,
- σ_θ = geometric standard deviation,
- ψ = inertial parameter.

III. FLOW PATTERN AROUND AN ISOLATED CYLINDER

For the two-dimensional irrotational flow of a non-viscous, incompressible fluid perpendicular to an infinite cylinder, the velocity of the fluid can be expressed in polar coördinates (18) by

$$\begin{aligned}
 v_r &= v_0(1 - (r_f^2/r^2)) \cos \theta \\
 v_\theta &= -v_0(1 + (r_f^2/r^2)) \sin \theta
 \end{aligned}
 \tag{1}$$

where r_f is the cylinder radius and v_0 is the upstream fluid velocity in the direction of $\theta = 0$; the origin of the coordinates is at the center of the cylinder. This potential flow velocity distribution is expected to hold at rather high values of the Reynolds number defined as

$$N_{\text{Re}} = \frac{d_f v_0 \rho}{\mu}$$

where d_f is the cylinder diameter, ρ is the gas density, and μ is the coefficient of viscosity of the gas.

At low Reynolds number the velocity field of the fluid around the cylinder depends primarily on the viscous forces, which are absent in ideal potential flow. Equations 1 are not expected to apply under conditions ordinarily encountered in filtration work. The solution of the force balance equations of a viscous fluid for flow around a cylinder has not been obtained, although some approximate solutions are available. Using the method of Oseen, which partially takes into account the inertial terms, Lamb (19) has obtained the velocity field around a stationary cylinder perpendicular to an incompressible viscous fluid:

$$\begin{aligned} v_r &= C_L \left[\left(1 - \frac{r_f^2}{r^2} \right) - 2 \ln \frac{r}{r_f} \right] \cos \theta \\ v_\theta &= C_L \left[\left(1 - \frac{r_f^2}{r^2} \right) + 2 \ln \frac{r}{r_f} \right] \sin \theta \end{aligned} \quad (2)$$

$$C_L = \frac{v_0}{2[2.00 - \ln N_{\text{Re}}]}$$

Equations 2 can be expected to hold close to the surface of the cylinder providing the Reynolds number is less than 1. For regions far from the cylinder, these equations are no longer valid. Lamb also obtained the total drag force per unit length of cylinder transverse to the flow as

$$F = 8\pi\mu C_L \quad (3)$$

Davies (7) has recently reviewed Lamb's solution. After criticizing some of Lamb's simplifying assumptions, he obtained an expression for the velocity which he considers to be more accurate than those given by Lamb. Davies also obtained equation 3 for the drag force per unit length of the cylinder. The equations for the velocity distribution of the fluid given by Davies are much more complicated than those given by Lamb.

To compare the flow pattern around a cylinder based on potential flow and viscous flow, Davies (8) has drawn the streamlines of flow transverse to a cylinder at N_{Re} equal to 2000, 10, and 0.2, respectively. The streamlines spread outwards to pass around the cylinder much more suddenly at high values of Reynolds numbers than at low values. In fact, the effect of the obstacle is hardly apparent at two cylinder diameters upstream for $N_{\text{Re}} = 2000$, but at $N_{\text{Re}} = 0.2$ there is a 3 per cent disturbance as far as 100 diameters ahead. Thus, with viscous flow, particles approaching in line with the cylinder begin to experience a slowing down and a gradual lateral displacement long before they are near, and are

much more apt to be displaced far enough sideways to miss it completely than at high speeds under equivalent circumstances.

IV. COLLECTION EFFICIENCY OF AN ISOLATED SINGLE CYLINDER

The collection efficiency of a single cylinder, η , is defined as the ratio of the cross-sectional area of the original stream from which the particles are removed to the projected area of the collector in the direction of the flow. In the following discussions the assumptions are made that all the particles which strike the collector adhere to its surface and the particles are too small to influence the flow pattern of the gas stream.

A. Collection by inertial impaction

Consider an aerosol stream moving in the x -direction towards a circular cylinder which is perpendicular to the direction of flow and effectively infinite in length. The motion of the aerosol particles approaching the cylinder will not be the same as that of the gas. The momentum of the particles makes them less subject to deviation from their course when the streamlines of flow spread sideways past the cylinder. Furthermore, the particles may be under the influence of external forces, electrical or gravitational.

Application of the law of motion to the movement of the particles gives

$$\frac{d(m\vec{u})}{dt} = \vec{F}_e - \frac{(\vec{u} - \vec{v})}{Z} \tag{4}$$

where m is the mass of the particle, \vec{u} and \vec{v} are the velocities of the particle and gas, respectively, \vec{F}_e is the vector sum of all the external forces, and the mobility Z is defined in such a way that the frictional forces of the gas opposing the particle motion give a resultant force of $-(\vec{u} - \vec{v})/Z$. For the ordinary case, the relative velocity between an aerosol particle and the gas is not too great, and Stokes' linear law of drag can be used. Then

$$Z = \frac{C}{3\pi\mu d_p} \tag{5}$$

where d_p is the diameter of the particle and C is Cunningham's (6) correction for particles having diameters of the order of the mean free path of the gas molecules, as the small particles have a tendency to slip between the gas molecules. In the absence of external forces, equation 4 takes the following form when Stokes' law is applicable:

$$\frac{C\rho_p d_p^2}{18\mu} \frac{d\vec{u}}{dt} = -(\vec{u} - \vec{v}) \tag{6}$$

where ρ_p is the particle density. By converting all the variables into dimensionless form, equation 6 can be expressed in rectangular coördinates as

$$\begin{aligned} 2\psi \frac{d^2\bar{x}}{d\bar{t}^2} + \frac{d\bar{x}}{d\bar{t}} - \bar{v}_x &= 0 \\ 2\psi \frac{d^2\bar{y}}{d\bar{t}^2} + \frac{d\bar{y}}{d\bar{t}} - \bar{v}_y &= 0 \end{aligned} \tag{7}$$

where

$$\psi = \frac{C\rho_p d_p^2 v_0}{18\mu d_f} = \text{inertial parameter}; \quad \tilde{x} = \frac{2x}{d_f}; \quad \tilde{y} = \frac{2y}{d_f};$$

$$\tilde{v}_x = \frac{v_x}{v_0}; \quad \tilde{v}_y = \frac{v_y}{v_0} \text{ and } \tilde{t} = \frac{2v_0 t}{d_f}$$

In the steady state, the velocity field of the fluid is a function of \tilde{x} , \tilde{y} , and N_{Re} only. A solution of equations 7 with the boundary conditions will give the position of the particle at any time \tilde{t} when the initial position of the particle is given. It is possible then to find the particle which, starting at infinity in the x -direction and at certain limiting distance from the axis of the cylinder, will just touch the surface of the cylinder. This limiting distance \tilde{y} is identical with the collection efficiency of the cylinder caused by inertial impaction and is a function of ψ and N_{Re} only.

Physically, the inertial parameter ψ represents the ratio of the force necessary to stop a particle travelling at a velocity v_0 in a distance $d_f/2$ to the fluid resistance acting on the particle moving according to Stokes' law with a relative velocity v_0 .

Because of the complex expressions for the fluid velocity, analytical solutions of the equations 7 to get the trajectory of a particle and thus the collection efficiency by inertia have not been obtained. Particle trajectories must be obtained by numerical stepwise solution of the equation.

Albrecht (1), Langmuir and Blodgett (22), and Stairmand (28) have made step-by-step calculations of the trajectories of the particles, assuming potential flow. Sell (27) used his own experimental streamlines around a cylinder in calculation. Landahl and Herrmann (20) used the flow field calculated by Thom (32) for $N_{Re} = 10$ for their step-by-step calculations of the theoretical efficiencies. The results of these calculations are in disagreement. The amount of the disagreement depends mainly on the nature of the flow field assumed and the accuracy of the calculations. Davies (8) also performed the calculations based on his viscous flow equations for $N_{Re} = 0.2$ (7). Figure 1 shows Davies' results calculated from his empirical equation (shown at $R = 0$). The efficiencies calculated by Davies are expected to be much lower than those given by others for potential flow.

Landahl and Herrmann (20) also gave experimental data on the impaction of atomized heterogeneous liquid droplets on wires. Wong (38) has studied the inertial impaction of homogeneous aerosols on cylinders in the range of N_{Re} from 13 to 330. His data check fairly well with the theoretical curve based on potential flow.

Langmuir and Blodgett (22) and Stairmand (28) have indicated that the critical value of ψ for inertial impaction on a cylinder is $1/6$, i.e., for ψ less than $1/6$, there is no collection of particles on a cylinder due to the inertial effect. Albrecht (1) gave the critical value as 0.09. Davies (8) did not mention a critical ψ in his calculation. On the basis of the equation for viscous flow, Langmuir (21) showed the critical ψ to be 0.27. Whether or not a critical ψ exists is an interesting

academic argument, but it is not of great practical importance since other mechanisms of collection usually enter at small values of ψ .

B. Collection by direct interception

A massless particle will have no inertia and its center will follow the fluid streamlines. If the particle has a finite diameter d_p , it will touch the collector when its center approaches within a distance $d_p/2$ of the collector surface. This effect is called direct interception. The maximum collection efficiency which can result from interception is $1 + (d_p/d_f)$, or $1 + R$. Using the potential flow equation 1, Ranz (25) has shown that the collection efficiency due to interception will be

$$\eta_0 = (1 + R) - \frac{1}{1 + R} \tag{8}$$

where $R = d_p/d_f =$ interception parameter.

In general, the interception collection efficiency will be a function of R and N_{Re} . For viscous flow (21), equation 2 gives the tangential velocity at $\theta = \pi/2$.

$$v_{\theta=\pi/2} = C_L \left[2 \ln \left(\frac{r}{r_f} \right) + \left(1 - \frac{r_f^2}{r^2} \right) \right] \tag{9}$$

The volumetric flow rate of the fluid Q passing the plane $\theta = \pi/2$ bounded by $r = r_f$ and $r = r_f + d_p/2$ per unit length of the cylinder is

$$Q = \int_{r_f}^{r_f+d_p/2} v_{\theta} dr = \frac{C_L d_f}{2} \left[2(1 + R) \ln (1 + R) - (1 + R) + \frac{1}{1 + R} \right] \tag{10}$$

If the particles are assumed to be massless so that they follow the fluid streamlines, the ratio of Q to $v_0 d_f/2$, the volumetric flow rate which passes a plane representing one half of the projected area of a unit length of the cylinder, is the efficiency of interception.

$$\eta_0 = \frac{1}{2[2.00 - \ln N_{Re}]} \left[2(1 + R) \ln (1 + R) - (1 + R) + \frac{1}{1 + R} \right] \tag{11}$$

Equation 11 was derived by Langmuir (21). Landahl and Herrman (20) have assumed arbitrarily that the efficiency of interception is equal to R . Rodebush (26) gave the same relation for the interception effect, but stated that it is applicable only in the limited case in which the cylinder diameter approaches zero.

Davies (8) calculated a curve for the efficiency of interception at $N_{Re} = 0.2$. While he did not give an equation, efficiencies read from his curve for values of R between 0.75 and 1.5 are almost identical with those calculated from equation 11 for $N_{Re} = 0.2$. For values of R less than 0.7, efficiencies given by Davies are higher than those calculated from equation 11.

C. Collection by Brownian diffusion

Particles of very small diameter show considerable Brownian movement and therefore do not move uniformly along the flow lines of the gas. This diffusion,

or migration of the particles from the flow line, tends to increase the number of particles collected by the cylinder. The effect will be most marked when the fluid velocity is low, since the particles remain longer in the neighborhood of the cylinder.

Einstein (9) showed by statistical analysis that the mean-square displacement of a particle in a given direction is related to the apparent diffusion coefficient D_{BM} in the following manner:

$$\bar{x}^2 = 2D_{BM}t \quad (12)$$

where \bar{x}^2 is the mean-square displacement of the particle in the x -direction in time t .

Einstein has also derived from Stokes' law an equation for the diffusion coefficient. When Cunningham's correction for slip of small particles between gas molecules is applied, the diffusion coefficient is given by equation 13,

$$D_{BM} = \frac{CkT}{3\pi\mu d_p} \quad (13)$$

where k is Boltzmann's constant and T is the absolute temperature.

No work has been done on solving the partial differential equations for diffusion in the moving gas near a cylinder to calculate exactly the number of aerosol particles that reach the collector surface. Langmuir (21) has contributed the following approximate solution based on the "random walk" theory. Statistically, the average absolute value of the displacement of a particle in time t along a certain direction is given by

$$\bar{x} = \left(\frac{4}{\pi} D_{BM}t \right)^{1/2} \quad (14)$$

The aerosol particle that passes near a cylinder along the flow lines does not stay in contact with the fiber for a definite time. The time that it takes a particle to pass from a point at $\theta = \pi/6$ from the upstream fluid direction to a point at $\theta = 5\pi/6$ through a point with distance x_0 away from the collector surface at $\theta = \pi/2$ may be taken as the "effective time" during which the diffusion occurs. The root-mean-square distance of the above movement from $\theta = \pi/6$ to $5\pi/6$ may be taken as the "effective distance" of the layer from which the particles diffuse. This effective distance and time should be related by equation 14. Any uncertainty in the determination of the effective distance and time will produce an uncertainty in the numerical coefficients of equations 15 and 16.

On the basis of equation 2 for viscous flow around a cylinder, Langmuir has calculated, for the first approximation of the effective distance and time,

$$x_e = 1.120x_0 \quad (15)$$

$$t = 0.139 \frac{d_f^2}{C_L x_0} \quad (16)$$

Equation 17, obtained by substituting equations 15 and 16 into equation 14, can be solved for x_0 , the effective thickness of the fluid layer at $\theta = \pi/2$ from which particles are removed by diffusion.

$$\frac{x_0}{d_f} = \frac{1}{2} \left[1.12 \frac{D_{BM}}{C_L d_f} \right]^{1/3} \tag{17}$$

If x_0 is much larger than is given by equation 17, a shorter time t and a greater distance x_e should be obtained and thus, by equation 14, there would not be time enough for particles in the thicker layer bounded by this flow line to diffuse to the cylinder. Similarly, if x_0 is too small, particles even from outside the selected layer will have had time to diffuse to the cylinder. Langmuir (21) states that the coefficient in equation 17 must be regarded as a rough approximation to the true value and is unlikely to be more than ± 20 per cent in error.

Following the derivation of equation 11 for the collection efficiency by interception, the Langmuir equation for the collection efficiency by diffusion is

$$\eta_0 = \frac{1}{2(2.00 - \ln N_{Re})} \left[2 \left(1 + \frac{2x_0}{d_f} \right) \ln \left(1 + \frac{2x_0}{d_f} \right) - \left(1 + \frac{2x_0}{d_f} \right) + \frac{1}{1 + \frac{2x_0}{d_f}} \right] \tag{18}$$

Equation 18 indicates that the collection efficiency by diffusion is a function of N_{Re} and $D_{BM}/v_0 d_f$ or D , the diffusion parameter. Figure 2 shows the collection efficiency calculated from equation 18 at $N_{Re} = 10^{-2}$ (shown at $R = 0$).

Johnstone and Roberts (14) and Ranz (25) have proposed applying the analogy of heat and mass transfer to the problem of collection by diffusion. The following equation was suggested by Ranz (25) for the fictitious film thickness for the particle diffusion.

$$\frac{d_f}{B_f} = \frac{1}{\pi} + 0.55 \left(\frac{d_f v_0}{D_{BM}} \right)^{1/3} \left(\frac{d_f v_0 \rho}{\mu} \right)^{1/6} \tag{19}$$

where B_f = fictitious mass transfer film thickness and d_f/B_f = Nusselt number for mass transfer.

The collection efficiency of a cylinder due to diffusion is

$$\eta_0 = \pi \left(\frac{D_{BM}}{v_0 d_f} \right) \left(\frac{d_f}{B_f} \right) \tag{20}$$

Although no experimental data are available to verify equation 19, the calculated collection efficiencies check fairly well with those calculated from equation 18 in the range of interest in filtration work.

Stairmand (28) used the same approach taken by Langmuir to calculate the diffusion collection efficiency. He assumed that the particles diffuse to the collector surface in a quiescent fluid within a time equal to $\pi d_f/2v_0$, and derived the following equation for the efficiency:

$$\eta_0 = \left(\frac{8D_{BM}}{v_0 d_f} \right)^{1/2} \tag{21}$$

Davies (8) arbitrarily assumed that the collection efficiency by diffusion is the same as that by the inertial effect when D and ψ have the same value. His assumption, however, seems to lack justification.

D. Collection by settling

Large particles under the force of gravity will settle on the collector surface. For a horizontal cylinder transverse to the flow, Ranz (25) has shown that the collection efficiency will be equal to the ratio of the free settling velocity u_g of the particle to the stream velocity v_0 . It constitutes a "settling parameter" G .

$$\eta_0 = \frac{u_g}{v_0} = \frac{Cd_p^2 \rho_p g}{18\mu v_0} = G \quad (22)$$

For a random cylinder transverse to the flow, the collection efficiency should be the efficiency calculated from equation 22 times the ratio of cross-sectional area projected in the vertical direction to that projected in the direction of the flow.

E. Collection by inertia and interception

The particles were considered as point masses in the calculation of collection efficiency due to inertial impaction. The finite size of the particles was only considered in the calculation of the fluid resistance encountered by them. Actually, the particles will be caught by the collector when their trajectories are less than

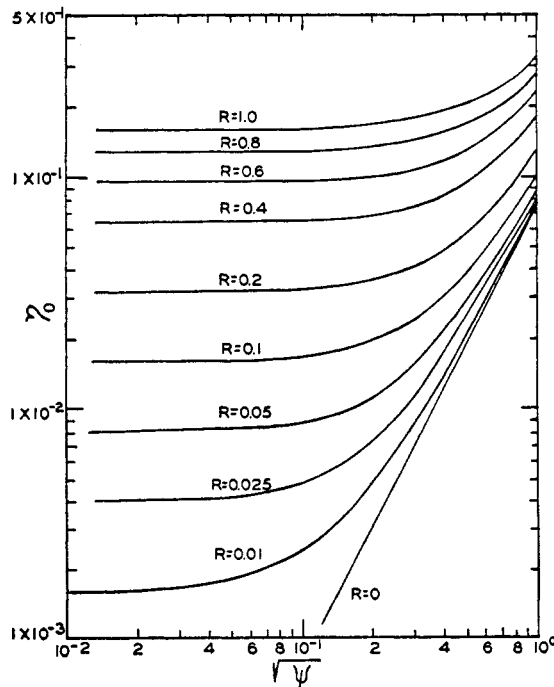


FIG. 1. Collection efficiency of an isolated cylinder by inertia and interception at $N_{Re} = 0.2$

$d_p/2$ away from the collector surface. This interception effect will change the boundary condition of the inertial impaction. The collection efficiency due to inertia and interception will be a function of ψ , R , and N_{Re} .

Davies (8) has calculated the collection efficiency due to inertia and interception at $N_{Re} = 0.2$. He gave the following equation to fit his results.

$$\eta_0 = 0.16[R + (0.50 + 0.8R)\psi - 0.1052R\psi^2] \tag{23}$$

Figure 1 shows the collection efficiency calculated from equation 23. It is interesting to note that the collection efficiency due to the combined effects of inertia and interception is higher than the sum of the efficiencies due to inertia and interception alone.

F. Collection by diffusion and interception

To consider the combined effects of interception and diffusion, any particle will be caught if its center comes within a distance of $d_p/2$ from the surface of the collector. The effective diffusion distance will be $x_0 - d_p/2$ instead of x_0 when diffusion alone is being considered. Langmuir (21) used the following equations instead of equations 15 and 16 as the effective distance and time for the calculation of the efficiency due to diffusion and interception.

$$x_e = 1.120 \left(x' - \frac{d_p}{2} \right) \tag{24}$$

$$t = 0.139 \frac{d_f^2}{C_L x'} \tag{25}$$

Substituting the above equations into equation 14, the following results:

$$\left[\frac{x'}{d_f} - \frac{1}{2} \frac{d_p}{d_f} \right]^2 \frac{x'}{d_f} = 0.14 \frac{D_{BM}}{C_L d_f} = \left(\frac{x_0}{d_f} \right)^3 \tag{26}$$

where x' = effective fluid layer thickness at $\theta = \pi/2$ around a cylinder from which all the aerosol particles are removed by the combined effects of diffusion and interception at certain D and N_{Re} , and

x_0 = effective layer thickness at $\theta = \pi/2$ around a cylinder from which all particles are removed by diffusion alone at the same D and N_{Re} as above.

The collection efficiency can be calculated by substituting x'/d_f , obtained from equation 26, into equation 18 instead of x_0/d_f . Efficiencies thus calculated at $N_{Re} = 10^{-2}$ have been plotted in figure 2. It is also found that the efficiency due to the combined effects is higher than the sum of the efficiencies due to the individual effects alone. No experimental work on the collection efficiency of an isolated cylinder by diffusion and interception has been reported. Langmuir's approximate solution needs experimental verification.

G. Overall collection efficiency

The overall collection efficiency is difficult to calculate. Davies (8) made the arbitrary assumption that the overall efficiency could be found by (1) calculating

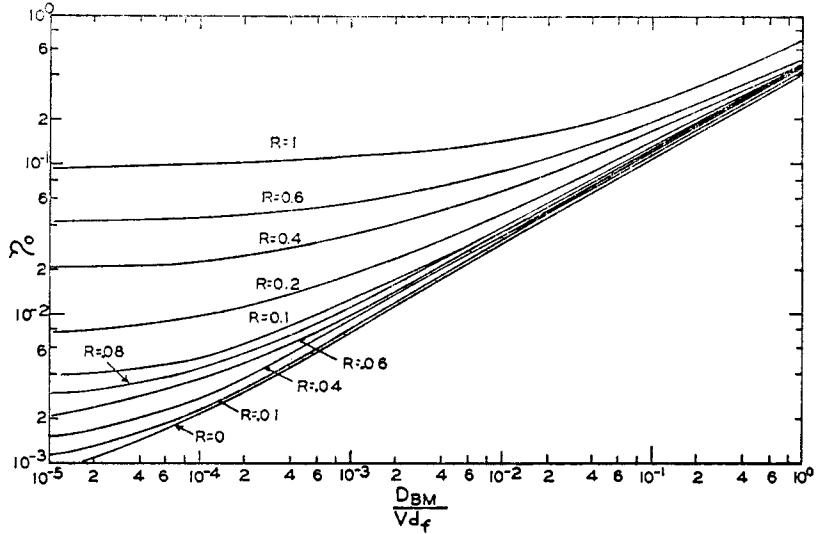


FIG. 2. Collection efficiency of an isolated cylinder by diffusion and interception at $N_{Re} = 10^{-2}$.

the inertia parameter ψ , the diffusion parameter D , and the interception parameter R , (2) taking the numerical sum of ψ and D , and (3) reading the inertia and interception collection efficiency curve as shown in figure 1 at particular $\psi + D$ and R instead of at certain ψ and R .

For a differential volume of fluid not too far from an infinite cylinder (5), the following equation gives the material balance on the aerosol particles.

$$\frac{\partial N}{\partial t} = -\text{div} (-D_{BM} \text{grad } N) - \text{div } \bar{v}N - \text{div} (\bar{u} - \bar{v})N \tag{27}$$

where N is the number concentration of particles. The term on the left represents the total rate of accumulation of particles, while the second, third, and fourth terms represent the rates of accumulation due to Brownian diffusion, flow, and relative velocity of particles $(\bar{u} - \bar{v})$, respectively. \bar{u} is found from the solution of equation 4 or 6. It has been stated that \bar{u} should be a function of \bar{x} , \bar{y} , ψ , and N_{Re} only. If only the steady state is considered, then equation 27 becomes

$$D_{BM} \left(\frac{\partial^2 N}{\partial x^2} + \frac{\partial^2 N}{\partial y^2} \right) - \left(\frac{\partial(\bar{u}_x N)}{\partial x} + \frac{\partial(\bar{u}_y N)}{\partial y} \right) = 0 \tag{28}$$

Analytical solution of equation 28 is generally impossible. However, by converting it into a dimensionless form, we can find the parameters that determine the particle concentration around a cylinder.

Let

$$\begin{aligned} \bar{x} &= \frac{2x}{d_f} & \bar{u}_x &= \frac{\bar{u}_x}{\bar{v}_0} \\ \bar{y} &= \frac{2y}{d_f} & \bar{u}_y &= \frac{\bar{u}_y}{\bar{v}_0} \end{aligned}$$

then equation 28 can be converted into

$$\frac{2D_{BM}}{v_0 d_f} \left(\frac{\partial^2 N}{\partial \tilde{x}^2} + \frac{\partial^2 N}{\partial \tilde{y}^2} \right) - \tilde{u}_x \frac{\partial N}{\partial \tilde{x}} - \tilde{u}_y \frac{\partial N}{\partial \tilde{y}} - N \left[\frac{\partial \tilde{u}_x}{\partial \tilde{x}} + \frac{\partial \tilde{u}_y}{\partial \tilde{y}} \right] = 0 \quad (29)$$

When there is no external force, solution of equation 29, including the interception effect as a boundary condition, shows that the number concentration of particles around a cylinder can be expressed as

$$N = f(\tilde{x}, \tilde{y}, N_{Re}, \psi, R, D) \quad (30)$$

The overall collection efficiency can be calculated from equation 30 and expressed as

$$\eta_0 = f[\psi, R, D, N_{Re}] \quad (31)$$

In case external forces are present, then the collection efficiency should also be a function of another parameter as G defined in equation 22 for gravitational force. The above derivation defines the parameters which determine the overall efficiency of a cylinder. Equation 31 has not been solved numerically. Chen (5) has made the assumption that the overall efficiency is equal to the sum of the efficiencies arising from the combined effects of inertia and interception and the combined effects of diffusion and interception. This is considered to be reasonable, particularly when either ψ or D is small.

H. Discussion

It has been shown by Tomotika and Aoi (35) that, even at Reynolds numbers as low as 0.05, eddies will be developed at the back of a cylinder. No attempt has been made to calculate the effect of these eddies on the overall collection efficiency.

An apparent slipping of the gas along a surface has been shown experimentally and theoretically. The thickness of the layer in which slip occurs is approximately equal to λ , the free path of the gas molecules. Langmuir (21) has given equations by which this slipping effect is approximately taken into account. Tsien (35a) has given a complete treatment of the slip flow.

V. FILTRATION OF AEROSOLS BY FIBROUS FILTERS

The theoretical prediction of penetration of aerosol particles through a fibrous filter consists of three steps:

1. Calculation of the collection efficiency of an isolated fiber at the same superficial velocity;
2. Finding the difference between the collection efficiency of an isolated fiber and an individual fiber in the filter due to the neighboring fiber interference effect; and
3. Finding the collection efficiency of a filter from the collection efficiency of the individual fibers.

Steps 2 and 3 will be discussed in the following sections. All of the discussion is based on aerosols of uniform particle size.

A. Relationship between the collection efficiency of fibrous filters and that of individual fibers

The orientation of fibers in ordinary filters can be considered to lie between two extreme cases. For the first case, the fibers are far apart and dispersed uniformly, and the neighboring fibers are staggered with respect to each other. For the second case, the fibers are so close together that the filter acts like a group of capillaries. Ordinary mats and papers behave more like the first case.

Considering a small volume element ($dA \cdot dL$) of a fibrous filter of the first kind with all the fibers randomly distributed in the plane transverse to the flow (5), the collection efficiency of a single fiber of size d_i in this particular filter is $\eta_{\alpha i}$. Assume the length of the fiber with diameter d_i in this filter to be l_i per unit volume of filter. Then the particles removed by all the fibers of different sizes in this small volume per unit time will be

$$vN \cdot dA \cdot dL \sum_i \eta_{\alpha i} d_i l_i$$

where N is the number concentration of the particles entering this small volume element, v is the average velocity of the gas stream in the filter, defined as v_s/ϵ , and ϵ is the porosity of the filter. The change in particle concentration due to passage through this small element should also be $-v_s dA \cdot dN$. Then

$$-dN/N = \frac{dL}{\epsilon} \sum_i \eta_{\alpha i} d_i l_i$$

or

(32)

$$-\ln N/N_0 = \frac{L}{\epsilon} \sum_i \eta_{\alpha i} d_i l_i$$

where L is the thickness of the filter. When measuring the fiber size distribution under a microscope or electron microscope, the longer the fiber the oftener it is seen. Thus, it can be assumed that the distribution function of the length of each fiber size is the same as the distribution of fiber diameter.

$$\frac{dl_i}{(\sum l_i)} = f(d_i)d(d_i) \quad (33)$$

where $(\sum l_i)$ = total length of fiber in unit volume of the filter and $f(d_i)d(d_i)$ = the distribution function of fiber size. Neglecting the end of the fiber, the total length of the fiber per unit volume of filter is related to the volume fraction of fiber α in the following way:

$$\sum_i \frac{\pi}{4} d_i^2 l_i = \alpha \quad (34)$$

Substitute equation 33 into equation 34. Then

$$\sum l_i = \frac{4\alpha}{\pi (d_f)_s^2} \quad (35)$$

where $(d_f)_s$ is the surface average fiber diameter. Equation 36, obtained by substituting equation 35 into equation 32, has the following form:

$$-\ln N/N_0 = \frac{4}{\pi} \frac{1 - \epsilon}{\epsilon} \frac{L}{(d_f)_s^2} \int \eta_{\alpha i} d_i f(d_i) d(d_i) \tag{36}$$

Unless the analytical expression of $\eta_{\alpha i}$ as a function of fiber size can be found, equation 36 has no practical significance. If the collection efficiency is independent of the fiber size, or inversely proportional to the fiber size, equation 36 becomes

$$-\ln N/N_0 = \frac{4}{\pi} \eta_{\alpha} \frac{1 - \epsilon}{\epsilon} \frac{(d_f)_{av} L}{(d_f)_s^2} \tag{37}$$

where η_{α} = collection efficiency of a single fiber in the filter calculated from the average fiber size.

Equation 37 was used by the author (5) to relate the single-fiber efficiency to the penetration of a filter. Although it is rather arbitrary to use the arithmetic average fiber size, the proper average size is probably close to the arithmetic average unless the geometric standard deviation of fiber size distribution σ_g is very large.

An equation similar to equation 37 was also derived by Langmuir (21) and Davies (8), considering the filter to be made of uniform fibers, which is not a realistic assumption.

$$-\ln N/N_0 = \frac{4}{\pi} \eta_{\alpha} \frac{1 - \epsilon}{\epsilon} \frac{L}{d_f} \tag{38}$$

B. The neighboring fiber interference effect

The collection efficiency of a single fiber in a filter is by no means the same as that of an isolated fiber at the same superficial velocity. Not only is the average velocity of the gas stream in a filter higher than the superficial velocity, but of even more importance is the change in the flow pattern around a fiber due to the presence of neighboring fibers. The presence of neighboring fibers will increase the collection efficiency of a single fiber. This increase will be a function of the volume fraction of fiber in the filter, and possibly of N_{Re} . It probably will be different for each collection mechanism. It may be expressed as

$$\eta_{\alpha} = \eta_0 f(\alpha, N_{Re}) \tag{39}$$

where η_{α} = collection efficiency of a single fiber in a filter with fiber volume fraction α at the superficial velocity v_s , and

η_0 = collection efficiency of an isolated fiber at the superficial velocity v_s .

As the volume fraction of fiber in a filter increases, the neighboring fiber interference effect increases the efficiency due to interception slowly but continuously. For the diffusion mechanism, the interference effect probably increases the efficiency to an asymptotic value. The squeeze of the streamlines around a

fiber will tend to increase the efficiency due to diffusion but the increase of average velocity in a filter will tend to decrease it. The presence of fibers upstream will increase the curvature of streamlines around a fiber downstream and will increase the collection efficiency due to inertial impaction.

Langmuir (21) assumed that the interference function in equation 39 can be found from pressure drop data. He considered diffusion and direct interception to be the only mechanisms of collection. The total drag force on an isolated cylinder transverse to the flow at low N_{Re} is $8\pi\mu C_L$, as shown in equation 3. From the theory of drag resistance, the pressure drop per unit thickness of a filter will be equal to the drag force on all the fibers in a unit volume of the filter. The drag force on the fiber in a filter is different from $8\pi\mu C_L$, but it may be expressed as $8\pi\mu C_{L\alpha}$. Then the pressure drop across a filter will be

$$\Delta p = \frac{32C_{L\alpha} \alpha \mu L}{d_f^2} \quad (40)$$

or

$$C_{L\alpha} = \frac{\Delta p d_f^2}{32\alpha\mu L} \quad (41)$$

where Δp = pressure drop across a filter.

Langmuir (21) made the assumption that the collection efficiency of an individual fiber in a filter can be calculated from equations 18 and 26 if $C_{L\alpha}$ is used instead of C_L .

Davies (8) assumed that the interference effect of a neighboring fiber is the same for different collection mechanisms. On the basis of Kovaszny's exact solution of viscous flow behind a two-dimensional grid (15), he calculated the collection efficiency due to interception of a single fiber with fiber fraction α to be

$$\eta_\alpha = R(0.16 + 10.9\alpha - 17\alpha^2) \quad (42)$$

Davies then made the assumption that the efficiency of collection of an individual fiber in a filter from all the collection mechanisms at $N_{Re} = 0.2$ can be expressed by combining equation 23 with 42 as follows:

$\eta_\alpha =$

$$(0.16 + 10.9\alpha - 17\alpha^2)[R + (0.5 + 0.8R)(\psi + D) - 0.1052R(\psi + D)^2] \quad (43)$$

After comparing the experimental data with the value predicted by equations 43 and 38, Davies concluded that, because of uneven fiber distribution and fiber aggregation, the diameter of the fiber used in equations 43 and 38 should be an effective one obtained from his empirical pressure-drop equation.

$$\Delta p = \frac{70\mu v_s L}{d_f'^2} \alpha^{1.5} (1 + 52\alpha^{1.5}) \quad (44)$$

where d_f' is the effective fiber diameter. Equation 44, obtained from experimental results, gives values of d_f' in close agreement with average fiber sizes

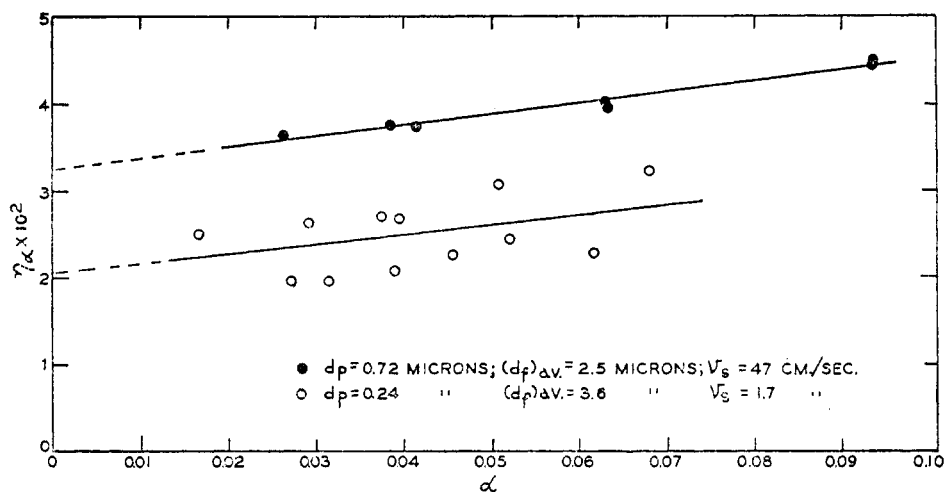


FIG. 3. The effect of neighboring fiber interference on the collection efficiency of a single fiber in the filter.

measured under the microscope for small values of α , but for larger values of α the effective size is usually greater than the measured average fiber size. Unfortunately, Davies did not publish his experimental data and there is some doubt as to the accuracy of his equations for the calculation of penetration of particles through a filter.

The author has attempted to find the interference effect experimentally (5). Penetration measurements were made on fiber mats of different porosity using homogeneous aerosols of a given particle size, fiber size, and superficial velocity. The individual fiber collection efficiencies η_α were calculated from the data by equation 37 and were plotted against α , as shown in figure 3. Although the experimental data scatter somewhat because of the non-uniformity of mats and the uncertainty of the particle size, the results indicate that the collection efficiency increases as the porosity decreases and can be correlated by the expression:

$$\eta_\alpha = \eta_0(1 + K\alpha) \quad (45)$$

For the eleven series of runs, K has an average of 4.5 and there seems to be little variation in its value even when different collection mechanisms are dominant. Extrapolation of equation 45 to α higher than 0.10 may result in large errors.

The interference effect given by equation 45 is much lower than that given by equation 42. Wong (38) has also found experimentally that equation 42 overestimates the interference effect. It will be shown later that Langmuir's theory also overestimates the interference effect.

C. Experimental results on penetration of aerosols through a filter

The experimental work reported in the literature on the filtration of aerosols is often difficult to interpret, because fiber size, porosity of the filter, size of

the particles, or the thickness of the filter are often not stated. Consequently, comparison between experimental results and the theoretical predictions usually cannot be made.

Lewis and Smith (23) gave experimental results on the filtration of an aerosol of unknown diameter through fiber mats. An equation was also derived for the collection efficiency of a mat. Direct interception and diffusion were considered as the only collection mechanisms. They assumed an approach similar to that of Langmuir for the isolated cylinder but assumed potential flow. Their experimental results cannot be compared with their equation.

Ramskill and Anderson (24) studied the filtration of homogeneous aerosols by different kinds of filter paper. The size of particles used was in general above 0.26 micron in diameter. The principal mechanisms of collection were found to be diffusion at low velocities, interception at moderate velocities, and inertial impaction at high velocities. However, the inertial impaction was found to play an important role at lower particle diameter than calculated by Albrecht (1) and Langmuir (21).

The filtration of homogeneous aerosols with particles as small as 0.04 micron through filter paper was studied by La Mer (17). Inertial impaction was also found to be important even for very small particles and the conclusion was drawn that the inertial effect overshadows the diffusion effect completely. The penetration of particles was found to increase monotonically with decreasing particle diameter when the velocity varies from 2.8 to 28 cm. per second.

Blasewitz *et al.* (2) measured the efficiency of filtration of heterogeneous aerosols by glass fiber mats. For each fiber size studied, the penetration of particles was correlated empirically as a function of mat bulk density, superficial velocity, and mat thickness.

D. G. Thomas (33) made penetration measurements on loose glass fiber mats, using a heterogeneous aerosol with average diameter of 0.4 micron. He used equation 38 to calculate the single-fiber collection efficiency and then attempted to compare this efficiency with theoretical isolated single-fiber efficiency. Some of his data at low velocity and small R compare favorably with the efficiency calculated from equation 18, considering diffusion as the only collection mechanism.

Wong (38) made a study of filtration by fiber mats using homogeneous aerosols at high velocities where inertial impaction is the controlling mechanism. His results indicate that the Davies theory of inertial impaction overestimates the efficiency. He found that varying the fiber volume fraction from 0.045 to 0.098 had no effect on the collection efficiency of a single fiber η_α . Equation 45 indicates that the efficiency should increase 20 per cent, while the Davies equation 42 indicates that it will increase 73 per cent.

D. J. Thomas (34) has made some penetration measurements on both loose mats and dense papers, using heterogeneous methylene blue aerosols with a mass median diameter of 0.5 micron. He did not try to correlate his results.

The author has made penetration measurements of homogeneous aerosols through "B" glass fiber mats ($(d_f)_{av.} = 2.5$, $(d_f)_s = 3.0$ microns) for particle

sizes between 0.15 and 0.72 micron with velocities ranging from 0.87 to 47.0 cm. per second (5). The porosities of the mats varied from 92 to 98 per cent. The results were correlated by using equations 37 and 45, with K equal to 4.5 to calculate the collection efficiency of an equivalent isolated fiber. The calculated isolated fiber efficiencies are plotted in figures 4 and 5 as a function of particle size and velocity, respectively. Figure 4 shows that, as the particle size decreases, the efficiency decreases at high velocities, remains essentially constant at medium velocities, and decreases at first but then increases at low velocities. Figure 5 indicates that, for velocities above 4 cm. per second, the efficiency always decreases as the particle size becomes smaller. However, for velocities below 4 cm. per second, there is a size of *minimum collection efficiency* at each velocity.

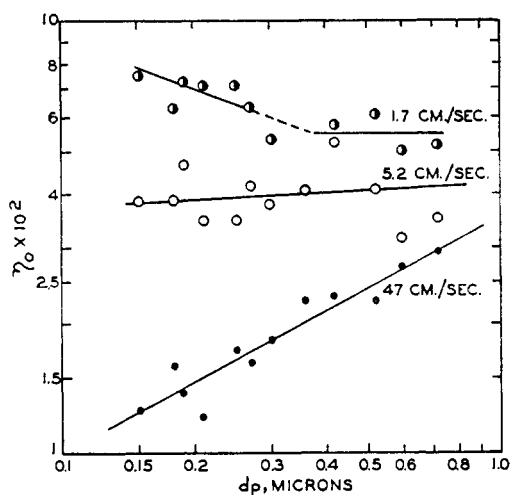


FIG. 4. Collection efficiency of an isolated 2.5-micron fiber calculated from particle penetration through fiber mats.

Qualitatively, the results obtained by the author, and those of Ramskill and Anderson (24), agree with the theory. Inertial impaction is important at high velocities, while diffusion is important at low velocities. The experimental results and the data in the literature were also compared with the theory, that is, the isolated single-fiber collection efficiencies calculated from experimental data by equations 37 and 45 were compared with the sum of the theoretical isolated fiber efficiencies from inertia and interception and due to diffusion and interception. As the theoretical efficiency of an isolated fiber from inertia and interception at low N_{Re} is not available, it was taken as the sum of the efficiencies by interception at the particular Reynolds number and by inertial impaction at $N_{Re} = 0.2$. Table 1 shows some of the calculations. The theory overestimates the efficiency at large values of ψ and underestimates it at large values of D . The theory and experimental results agree well as to the velocity at which the collection efficiency remains essentially constant, and the velocity at which it first

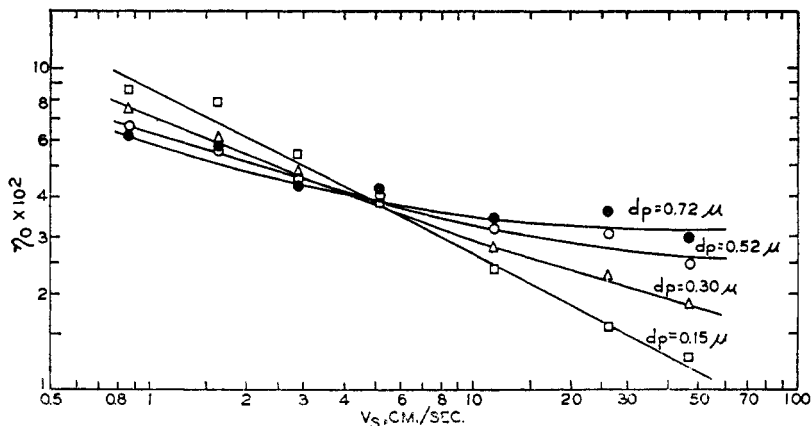


FIG. 5. Collection efficiency of an isolated 2.5-micron fiber calculated from particle penetration through fiber mats.

decreases and then increases as the particle size decreases. The discrepancies between the theory and experiment could be due either to the inaccuracy of the theoretical isolated fiber efficiency or to the experimental data or to the theory of collection efficiency of a filter. More theoretical and experimental work is needed before better comparisons can be made.

D. Particle size for maximum penetration

Theoretically, the efficiency of collection by diffusion decreases and that by inertial impaction increases as the velocity and particle size increase. Thus, it appears that there should be a particle size with maximum penetrating power for a given fiber size and at a given velocity. Limited experimental results of two studies (17, 24) have indicated that no such particle size of maximum penetration exists. In both cases, rather dense paper was used and the lowest velocity studied was 2.7 cm. per second. The author found no maximum penetration particle size for velocities above 4 cm. per second when using fiber mats with average fiber size of 2.5 microns. For velocities below 4 cm. per second, there does appear to be a maximum penetration size. Theoretical calculations by the author also indicate that, for the particle size range studied, a maximum penetration size exists only when the velocity is below 5 cm. per second.

It would be easier to find a particle size of maximum penetration by using a mat made of large fibers instead of small fibers, as the maximum penetration size should exist at higher velocities for mats of large fibers. As the inertial impaction persists to lower velocities for a dense paper, it is necessary to go to very low velocities to find a maximum penetration particle size when a paper is used instead of a loose mat.

VI. PRESSURE DROP ACROSS FIBROUS FILTERS

A. Channel theory

Two different approaches have been followed in the study of the pressure drop across fibrous media. It is customary to consider porous beds as a system of

TABLE 1

Comparison of experimental collection efficiency of single fibers in filter with theory

v_s	ψ	D	η_0 (Theory)	η_0 (Experiment)
1. Chen's data (5): $(d_f)_{av.} = 2.5 \mu$; $(d_f)_s = 3.0 \mu$				
(a) $d_p = 0.52 \mu$; $R = 0.21$				
<i>cm./sec.</i>				
46.9	0.199	5.10×10^{-5}	3.58×10^{-2}	2.45×10^{-2}
11.7	4.96×10^{-2}	2.06×10^{-4}	2.18	3.12
5.21	2.22×10^{-2}	4.60×10^{-4}	2.12	4.08
1.65	7.00×10^{-3}	1.46×10^{-3}	2.51	5.60
0.87	3.70×10^{-3}	2.76×10^{-3}	3.05	6.55
(b) $d_p = 0.30 \mu$; $R = 0.12$				
46.9	7.88×10^{-2}	1.06×10^{-4}	1.59×10^{-2}	1.82×10^{-2}
11.7	1.97×10^{-2}	4.28×10^{-4}	1.38	2.75
5.21	8.80×10^{-3}	9.55×10^{-4}	1.65	3.95
1.65	2.78×10^{-3}	3.03×10^{-3}	2.18	5.95
0.87	1.47×10^{-3}	5.73×10^{-3}	2.86	7.35
(c) $d_p = 0.15 \mu$; $R = 0.06$				
46.9	2.80×10^{-2}	3.02×10^{-4}	0.96×10^{-2}	1.25×10^{-2}
11.7	6.98×10^{-3}	1.22×10^{-3}	1.22	2.35
5.21	3.12×10^{-3}	2.72×10^{-3}	1.88	3.80
1.65	9.88×10^{-4}	8.62×10^{-3}	2.85	7.80
0.87	5.20×10^{-4}	1.63×10^{-2}	4.04	8.45
2. Ramskill and Anderson's data (24)				
(a) $d_f = 2.0 \mu$; $d_p = 0.30 \mu$; $\alpha = 0.098$; $L = 0.0735 \text{ cm.}$; $R = 0.15$				
8.4	1.78×10^{-2}	7.44×10^{-4}	1.8×10^{-2}	4.80×10^{-2}
20.0	4.24×10^{-2}	3.33×10^{-4}	1.6	4.23
36.0	7.61×10^{-2}	1.85×10^{-4}	1.8	4.12
70.0	1.49×10^{-1}	9.48×10^{-5}	3.6	4.40
126	2.67×10^{-1}	5.27×10^{-5}	3.7	5.36
(b) $d_f = 3.0 \mu$; $d_p = 0.30 \mu$; $\alpha = 0.17$; $L = 0.077 \text{ cm.}$; $R = 0.10$				
5.6	7.9×10^{-3}	7.55×10^{-4}	1.2×10^{-2}	0.84×10^{-2}
20	2.82×10^{-2}	2.10×10^{-4}	0.98	0.63
80	1.13×10^{-1}	5.23×10^{-5}	2.3	0.60
125	1.76×10^{-1}	3.36×10^{-5}	2.3	0.73
215	3.03×10^{-1}	1.96×10^{-5}	2.9	1.28
3. Data of Thomas (33): $(d_f)_{av.} = 10.6 \mu$; $(d_f)_s = 11.3 \mu$; $d_p = 0.40 \mu$; $\alpha = 0.032$; $L = 0.274 \text{ cm.}$; $R = 0.038$				
1.22	1.00×10^{-3}	6.65×10^{-4}	7.3×10^{-3}	8.16×10^{-3}
3.04	2.58×10^{-3}	2.65×10^{-4}	4.4	5.13
9.1	7.42×10^{-3}	8.90×10^{-5}	3.2	2.94
21.2	1.73×10^{-2}	3.82×10^{-5}	4.2	1.98
91.0	7.42×10^{-2}	8.90×10^{-6}	6.4	1.25

interconnected channels and the pressure drop for viscous flow through them is based on D'Arcy's equation

$$\Delta p = k_0 v_s \mu L \quad (46)$$

where k_0 is a constant. A theoretical treatment by Kozeny (16), who introduced the concept of the hydraulic radius, and a subsequent modification of Kozeny's equation by Carman (4) enable the constant in equation 46 to be related to the physical constants of the bed by the so-called Kozeny-Carman equation

$$\Delta p = \frac{k_1 v_s \mu S_0^2 (1 - \epsilon)^2 L}{\epsilon^3} \quad (47)$$

where $k_1 = \text{constant}$ and $S_0 = \text{specific surface of the packing material}$.

The Kozeny-Carman equation, either in the above form or in some modified form to introduce shape and orientation factors, has been applied to fibrous media by Wiggins, Campbell, and Maass (37), Fowler and Hertel (12), Sullivan and Hertel (30), and Sullivan (29).

A review of this approach to the problem has been given by Sullivan and Hertel (31), who express the equation for the pressure drop across a fibrous bed as

$$\Delta p = \frac{k_2 \mu v_s L S_0^2 (1 - \epsilon)^2}{k_3 \epsilon^3} \quad (48)$$

where $k_2 = \text{a shape factor, which has the same value for all geometrically similar channels, and}$

$k_3 = \text{an orientation factor, which has the value of 1 and 0.5 for flow parallel to the fibers and for flow perpendicular to the fibers, respectively.}$

k_2 has been found not to be a constant, as it increases with increase in porosity. Equation 48 is not expected to hold for filters with porosity higher than 0.88.

Langmuir (21) gave an expression for the pressure drop across a fiber mat. He derived first an expression for the resistance of evenly spaced cylindrical fibers with their axes parallel to the direction of flow and then introduced a numerical factor B to take into account the actual geometry of the filters, i.e., fibers not uniformly distributed, crossing one another at all angles, and lying mainly parallel to the surface of the filter and perpendicular to the direction of flow. His equation is

$$\Delta p = \frac{16B\mu\alpha\phi v_s L}{d_f^2} \quad (49)$$

where $B = \text{a numerical factor of the order of unity whose value depends on the geometry of the filter and } \phi = \text{a function of } \alpha \text{ defined by the expression}$

$$\frac{1}{\phi} = -\ln \alpha + 2\alpha - \frac{\alpha^2}{2} - \frac{3}{2}$$

Davies (8) has shown by the method of dimensional analysis that, if D'Arcy's law holds, then

$$\Delta p = \frac{\mu v_s L}{d_f^2} f(\alpha) \tag{50}$$

From measurements on a large number of different fibrous materials he found that

$$f(\alpha) = 64\alpha^{1.5}(1 + 56\alpha^3) \tag{51}$$

with only a small deviation of the data, considering the range of materials and porosities covered.

B. Drag theory

Brinkman (3) has shown that the pressure-drop equation based on the channel theory is not applicable for highly porous media. Since the porosities of ordinary filters are above 75 per cent, the application of channel theory is thus in doubt. Iberall (13) has followed another approach in which the pressure drop across a unit thickness of filter is the total drag force on the fibers in a unit volume of the filter. He assumed an equipartition of the fibers in the three perpendicular directions. From Emersleben's paper (10) on the viscous drag of a fluid on a special array of cylinders, Iberall estimated the drag force on a circular fiber surrounded by similar fibers all oriented along the direction of flow and with moderate separations to be:

$$F = 4\pi\mu v \tag{52}$$

For the drag force on the fibers with axes perpendicular to the direction of flow, he used equation 3 from Lamb.

By simple addition of the three pressure drops necessary to overcome the drag of the three sets of fibers, the following equation was obtained.

$$\Delta p = \frac{16\mu v_s L}{3d_f^2} \frac{1 - \epsilon}{\epsilon} \frac{4 - \ln N_{Re}}{2 - \ln N_{Re}} \tag{53}$$

Analysis of experimental data for glass fibers showed, however, that the results were best fitted by the equation:

$$\Delta p = \frac{9.4\mu v_s L}{d_f^2} \frac{1 - \epsilon}{\epsilon} \frac{2.4 - \ln N_{Re}}{2.0 - \ln N_{Re}} \tag{54}$$

The interference effect between neighboring fibers was not considered by Iberall. On the basis of the drag theory, Wong (38) used an effective drag coefficient C_{De} in his derivation to account for the effects of non-perpendicular fibers, fiber interference, end of fibers, and non-uniform fiber distributions. His equation is

$$\Delta p = \frac{2}{\pi} \frac{C_{De} \rho v_s^2 \alpha L}{d_f} \tag{55}$$

The effective drag coefficient C_{De} was found to be higher than that calculated from Lamb's equation for isolated cylinders, particularly at low N_{Re} .

The drag force on a unit length of fiber with diameter d_i transverse to the flow in a filter with fiber volume fraction α can be defined as

$$F_i = \frac{C_{D\alpha i} \rho v^2}{2 g_c} d_i \quad (56)$$

where $g_c = \text{conversion factor} = 980 \frac{(\text{g. mass})(\text{cm.})}{(\text{g. force})(\text{sec.}^2)}$,

$F_i = \text{drag force per unit length of fiber with diameter } d_i, \text{ and}$

$C_{D\alpha i} = \text{drag coefficient for fiber diameter } d_i \text{ in filter with fiber volume fraction } \alpha.$

Following the derivation of the collection efficiency of a filter, given above as equation 37, the author has derived (5) the following equation by summing up all the drag forces on the fibers in a unit volume of filter as the pressure drop across unit thickness of filter.

$$\Delta p = \frac{2\alpha\rho v^2 L}{\pi g_c (d_f)_s^2} \int C_{D\alpha i} d_i f(d_i) d(d_i) \quad (57)$$

When the drag coefficient is inversely proportional to the Reynolds number, the following equation can be obtained from equation 57:

$$\Delta p = \frac{2}{\pi} \frac{\alpha\rho v^2}{g_c} C_{D\alpha} \frac{(d_f)_{av.} L}{(d_f)_s^2} \quad (58)$$

where $C_{D\alpha} = \text{drag coefficient of a fiber of average size } (d_f)_{av.} \text{ in a filter with fiber volume fraction } \alpha.$

The drag coefficient of a fiber in the filter would not be the same as that of an isolated fiber, as assumed by Iberall. White (36) has shown that the drag coefficient of a cylinder moving in a tank does not obey the equation of Lamb given below for an isolated cylinder calculated from equation 3.

$$C_D = \frac{8\pi}{N_{Re}(2.00 - \ln N_{Re})} \quad (59)$$

Instead he found that the drag coefficient is inversely proportional to N_{Re} and could be correlated by the following equation:

$$\frac{C_{D\alpha}}{2} \cdot N_{Re} = \frac{k'}{\ln k'' d_b/d_f} \quad (60)$$

where $d_b = \text{the distance between the cylinder and the boundary. At low } N_{Re}, \text{ the value given by equation 60 is much higher than that predicted by equation 59. At high } N_{Re}, \text{ the value given by equation 60 approaches that given by Lamb's equation, since the effect of the outer boundary diminishes.}$

The author (5) has assumed that the neighboring fibers act like a boundary around a given fiber, and the ratio of interfiber distance to the fiber diameter will determine the drag coefficient for a fiber in a filter, particularly at a low Reynolds number. Assuming that a filter has the same interfiber distance in all

three directions and the fibers in each layer form a screen, the following equation gives the ratio of the interfiber distance to the fiber diameter for this particular model:

$$d_b/d_f = \left[\frac{2}{\pi} \alpha \right]^{-1/2} - 1 \tag{61}$$

where d_b = interfiber distance. For ordinary filters, the ratio of interfiber distance to the fiber diameter will probably be inversely proportional to the square root of α . Following equation 60, the drag coefficient of a fiber in filters of different porosity should be correlated by the following equation:

$$\frac{C_{D\alpha}}{2} \cdot N_{Re} = \frac{k_4}{\ln k_5 \alpha^{-0.5}} \tag{62}$$

$$\Delta p = \frac{4}{\pi} \frac{k_4}{\ln k_5 \alpha^{-0.5}} \frac{\alpha}{1 - \alpha} \frac{\mu v_s L}{(d_f)_s^2} \tag{63}$$

From equations 58 and 62, $\frac{C_{D\alpha}}{2} \cdot N_{Re}$ calculated from the data on one filter should be independent of Reynolds number. Values from different filters should be correlated by equation 62. For filters containing fibers with different orientations, and made by different techniques, the constants k_4 and k_5 in equation 62 may be different.

C. Experimental results

Considerable experimental work (2, 5, 11, 24, 33, 38) has been reported on the pressure drop across filter mats. In most cases, however, the results only show the proportionality to the superficial velocity and thickness of the filter, and empirical exponential function of porosity.

The author (5) has correlated by equations 58 and 62 all the pressure-drop data that have been reported. The group $\frac{C_{D\alpha}}{2} \cdot N_{Re}$ is plotted against N_{Re} in figures 6 and 7, which also shows equation 59 for an isolated cylinder. The drag

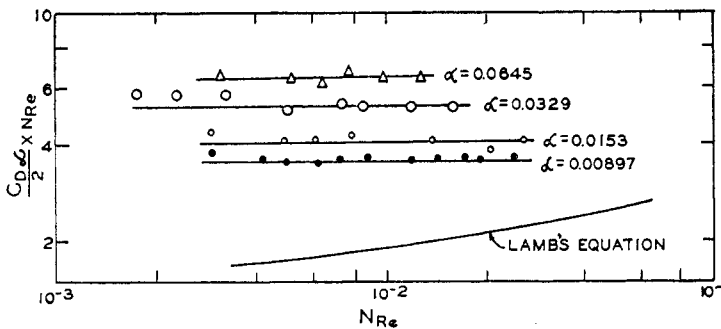


FIG. 6. Drag coefficients of a single fiber in fibrous media (5) (glass fiber mats with $(d_f)_{av} = 0.94$ micron).

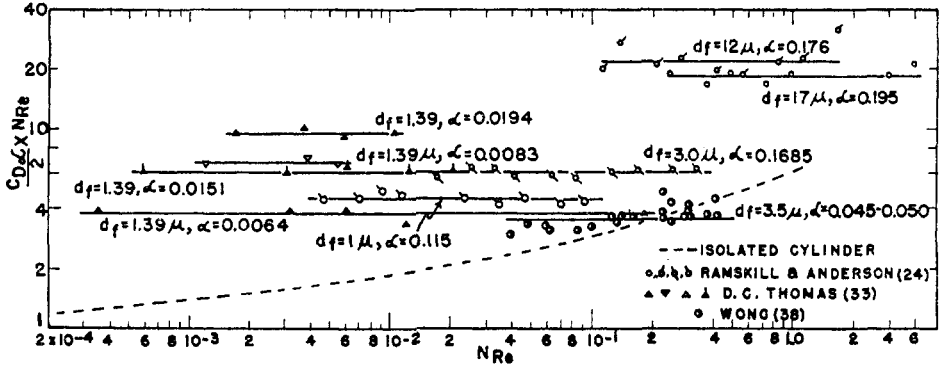


FIG. 7. Drag coefficients of a single fiber in fibrous media

coefficient of a single fiber in the filter is usually higher than that predicted by equation 59. $\frac{C_{D\alpha}}{2} \cdot N_{Re}$ calculated from data for one filter is independent of N_{Re} and is a function of α only. Thus, the flow around a fiber in a filter differs considerably from the flow around an isolated cylinder.

The experimental results are well correlated by equation 62, as shown in figure 8. They definitely indicate that neighboring fibers act as boundaries around a fiber. Most of the data in figure 8 can be fitted with k_4 and k_5 equal to 6.1 and 0.64, respectively. The scattering of the data might be caused by

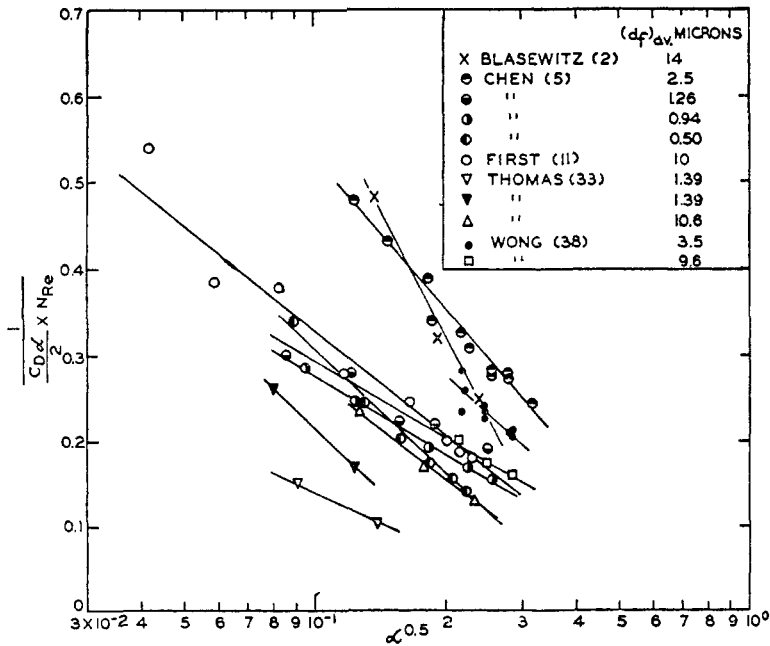


FIG. 8. Effect of fiber interference on the drag coefficients of a single fiber in the fibrous media.

TABLE 2

Critical α below which there is no neighboring fiber interference effect

N_{Re}	α (Critical)	N_{Re}	α (Critical)
10^{-4}	7.8×10^{-6}	10^{-1}	6.3×10^{-3}
10^{-3}	7.1×10^{-5}	0.5	3.0×10^{-2}
10^{-2}	6.8×10^{-4}	1	5.9×10^{-2}

inaccuracy of measurements of pressure drop and fiber size and different techniques of making the filters.

At each N_{Re} there is an α at which the drag coefficient given by equation 62 is the same as that given by equation 59 for an isolated cylinder. Below this critical value, the effect of neighboring fiber boundaries diminishes, and equation 59 should be used for the calculation of the drag coefficient of the fiber in the filter. If k_4 and k_5 are equal to 6.1 and 0.64, respectively, table 2 gives the values of critical α at different N_{Re} below which equation 59 should be used.

Table 2 agrees with Wong's results (38) very well. He found that for filters with α between 0.04 and 0.08, the drag coefficient is linear with N_{Re} up to a value of 0.6. For N_{Re} values greater than 0.6, the experimental curve exhibits a curvature more or less similar to that of equation 59.

By comparing equations 45 and 62, it can be seen that the interference effects increase the pressure drop much more than they increase the collection efficiency. It would be rather difficult to correlate collection efficiency directly with the pressure drop as was done by Langmuir (21).

If all the pressure-drop equations given in the literature are rearranged into a form comparable with equations 58 and 62, the drag coefficients of a single fiber in the filter with fiber volume fraction α are expressed as follows:

Kozeny-Carman, equation 48:
$$\frac{C_{D\alpha}}{2} \cdot N_{Re} = 4\pi \frac{k_2}{k_3} \cdot \frac{\alpha}{(1 - \alpha)^2} \tag{64}$$

Davies, equation 51:
$$\frac{C_{D\alpha}}{2} \cdot N_{Re} = 16\pi(1 - \alpha)\alpha^{0.5}(1 + 56\alpha^3) \tag{65}$$

Davies, equation 44:
$$\frac{C_{D\alpha}}{2} \cdot N_{Re} = 17.5\pi(1 - \alpha)\alpha^{0.5}(1 + 52\alpha^{1.5}) \tag{66}$$

Iberall, equation 52:
$$\frac{C_{D\alpha}}{2} \cdot N_{Re} = \frac{4\pi}{3} \cdot \frac{4 - \ln N_{Re}}{2 - \ln N_{Re}} \tag{67}$$

Iberall, equation 53:
$$\frac{C_{D\alpha}}{2} \cdot N_{Re} = 2.4\pi \frac{2.4 - \ln N_{Re}}{2.0 - \ln N_{Re}} \tag{68}$$

Langmuir, equation 49:
$$\frac{C_{D\alpha}}{2} \cdot N_{Re} = 4\pi B(1 - \alpha)\phi \tag{69}$$

Iberall's equations obviously cannot fit the data, since they do not take into account the neighboring fiber interference effects.

TABLE 3
 Values of $\frac{C_{D\alpha}}{2} \cdot N_{Re}$ as calculated from different equations

α	Kozeny-Carman Equation 64	Davies Equation 65	Davies Equation 66	Langmuir Equation 69	Chen Equation 62
0.001	0.075	1.58	1.73	2.32	2.03
0.005	0.374	3.53	3.86	3.30	2.77
0.01	0.760	4.95	5.42	4.00	3.29
0.05	4.16	10.6	12.0	7.46	5.80
0.10	9.20	15.1	18.2	11.4	8.67
0.15	15.6	19.6	26.2	15.6	12.2
0.25	33.5	35.4	54.4	26.6	25.2

Table 3 gives values of the $\frac{C_{D\alpha}}{2} \cdot N_{Re}$ at different values of α , as predicted from the above equations and equation 62. In the calculations k_2/k_3 was taken as 6.0, as found by Sullivan and Hertel for glass fibers perpendicular to the flow. The coefficient B in Langmuir's equation was taken as 1. The constants k_4 and k_5 in equation 62 were taken as 6.1 and 0.64, respectively.

The values given by Langmuir's equation agree fairly well with those calculated from equation 62.

VII. THE FILTRATION CRITERION

The criterion for judging a filter is expressed by

$$\gamma = \frac{-\ln N/N_0}{\Delta p} = \frac{2\eta_\alpha(d_f)_{av.}}{C_{D\alpha} \cdot N_{Re} \cdot \mu v_s} = \frac{\eta_0(d_f)_{av.}(1 + 4.5\alpha) \ln(k_5 \alpha^{-0.5})}{k_4 \mu v_s} \quad (70)$$

The higher the value of γ , the better the filter.

The following conclusions can be drawn from equation 70:

(1) For the same d_f , d_p , and v_s : The lower the value of α , the higher the value of γ .

(2) For the same d_p , v_s , and α : At low velocities, diffusion is important, and the larger the fiber size, the higher the value of γ . At high velocities, inertia is important, and γ remains essentially constant. At medium velocities, interception is important, and the smaller the fiber size, the higher the value of γ .

(3) For the same d_f , d_p , and α : The value of γ decreases at first, remains fairly constant, and then increases as the velocity increases.

(4) For the same d_f , v_s , and α : At high velocities, the value of γ increases with increasing d_p . At medium velocities, the value of γ remains essentially constant. At low velocities, the value of γ increases with decreasing d_p .

Acknowledgment is made to Professor H. F. Johnstone for the advice, assistance, and encouragement he has given to the author. Thanks are also due to Dr. R. K. Finn for his careful review and criticism of the manuscript.

VIII. REFERENCES

- (1) ALBRECHT, F.: *Physik. Z.* **32**, 48 (1931).
- (2) BLASEWITZ, A. G., CARLISLE, R. V., JUDON, B. F., KATZER, M. F., KURTZ, E. F., SCHMIDT, W. C. AND WEIDENBAUM, B.: Report HW-20847, Hanford Works, U. S. Atomic Energy Commission (1951).
- (3) BRINKMAN, H. C.: *Appl. Sci. Research* **A1**, 27 (1949).
- (4) CARMAN, P. C.: *Trans. Inst. Chem. Engrs. (London)* **15**, 150 (1937).
- (5) CHEN, C. Y.: Annual Report, Contract DA18-108-CML-4789, Engineering Experiment Station, University of Illinois (January 30, 1954).
- (6) CUNNINGHAM, E.: *Proc. Roy. Soc. (London)* **A83**, 357 (1910).
- (7) DAVIES, C. N.: *Proc. Phys. Soc. (London)* **B63**, 268 (1950).
- (8) DAVIES, C. N.: *Proc. Inst. Mech. Engrs. (London)* **B1**, 185 (1952).
- (9) EINSTEIN, A.: *Ann. Physik* **17**, 549 (1905); **19**, 371 (1906).
- (10) EMERSLEBEN, O.: *Physik. Z.* **26**, 601 (1925).
- (11) FIRST, M. W.: "Air Cleaning Studies," School of Public Health, Harvard University, Progress Report, Contract No. AT-(30-1)-841, N. Y. Operations Office, U. S. Atomic Energy Commission, No. 1581 (1951).
- (12) FOWLER, J. L., AND HERTEL, K. L.: *J. Appl. Phys.* **11**, 496 (1940).
- (13) IBERALL, A. S.: *J. Research Natl. Bur. Standards* **45**, 398 (1950).
- (14) JOHNSTONE, H. F., AND ROBERTS, M. H.: *Ind. Eng. Chem.* **41**, 2417 (1949).
- (15) KOVASZNAY, L. I. G.: *Proc. Cambridge Phil. Soc.* **44**, 58 (1948).
- (16) KOZENY, J.: *Wasserkraft u. Wasserwirtsch.* **22**, 67, 86 (1927).
- (17) LA MER, V. K.: Report No. NYO-512, Columbia University (1951).
- (18) LAMB, H.: *Hydrodynamics*, 6th edition, p. 77. Cambridge University Press, London (1932).
- (19) Reference 18, pp. 606-16.
- (20) LANDAHL, H. D., AND HERRMANN, R. G.: *J. Colloid Sci.* **4**, 103 (1949).
- (21) LANGMUIR, I.: OSRD Report No. 865 (1942).
- (22) LANGMUIR, I., AND BLODGETT, K. B.: Report No. RL-225, General Electric Research Lab., Schenectady, N. Y. (1944-1945).
- (23) LEWIS, W. K., AND SMITH, J. M.: OSRD Report No. 1251 (1942).
- (24) RAMSKILL, E. A., AND ANDERSON, W. L.: *J. Colloid Sci.* **6**, 416 (1951).
- (25) RANZ, W. E.: Tech. Report No. 3, Contract AT-(30-3)-28, University of Illinois (1951).
- (26) RODEBUSH, W. H.: "Filtration of Aerosols" in *Handbook of Aerosols*, p. 117. U. S. Atomic Energy Commission, Washington, D. C. (1950).
- (27) SELL, W.: *Forsch. Gebiete Ingenieurw.* **2**, Forschungsheft 347 (August, 1931).
- (28) STAIRMAND, C. J.: *Trans. Inst. Chem. Engrs. (London)* **28**, 130 (1950).
- (29) SULLIVAN, R. R.: *J. Appl. Phys.* **12**, 503 (1941).
- (30) SULLIVAN, R. R., AND HERTEL, K. L.: *J. Appl. Phys.* **11**, 761 (1940).
- (31) SULLIVAN, R. R., AND HERTEL, K. L.: *Advances in Colloid Science*, Vol. I, p. 37. Interscience Publishers, Inc., New York (1942).
- (32) THOM, A.: *Proc. Roy. Soc. (London)* **A141**, 651 (1933).
- (33) THOMAS, D. G.: Ph.D. Thesis in Chemical Engineering, Ohio State University 1953.
- (34) THOMAS, D. J.: *J. Inst. Heating Ventilating Engrs. (London)* **20**, No. 201, 35 (1952).
- (35) TOMOTIKA, S., AND AOI, T.: *Quart. J. Mech. and Appl. Math.* **3**, 140 (1950).
- (35a) TSIEN, H. S.: *J. Aeronaut. Sci.* **13**, 653 (1946).
- (36) WHITE, C. M.: *Proc. Roy. Soc. (London)* **A186**, 472 (1946).
- (37) WIGGINS, E. J., CAMPBELL, W. B., AND MAASS, O.: *Can. J. Research* **17**, 318 (1939).
- (38) WONG, J. B.: Ph.D. Thesis in Chemical Engineering, University of Illinois, 1954.